Journal of Materials Chemistry A

PAPER

View Article Online
View Journal | View Issue

Cite this: J. Mater. Chem. A, 2016, 4, 3546

New insights into exciton binding and relaxation from high time resolution ultrafast spectroscopy of $CH_3NH_3PbI_3$ and $CH_3NH_3PbBr_3$ films†

Vinay sharma, Sigalit Aharon, Itay Gdor, Chunfan Yang, Lioz Etgar and Sanford Ruhman*

Received 26th November 2015
Accepted 28th January 2016

DOI: 10.1039/c5ta09643j

www.rsc.org/MaterialsA

High time resolution broadband pump-probe experiments on $CH_3NH_3PbI_3$ and $CH_3NH_3PbBr_3$ films are described. The improved time resolution delineates instantaneous and delayed relaxation related effects on sample absorption and assists in clarifying controversial assignment of the underlying mechanisms. Analysis of the data in terms of finite difference spectra and spectral band integrals reveals that photoexcitation is high in the inter-band continuum leading to partial bleaching and red-shifts of the exciton band just below the absorption-edge instantaneously. Increased pump intensity saturates the exciton bleach and progressively reduces inter-band absorption in a broad range extending from the band edge to higher photon energies. Both effects are attributed to reduced Coulomb enhancement due to hot carrier screening. The spectral extent of the inter-band absorption attenuation provides estimated binding energies in the range of 20–30 meV in both materials. Sub-picosecond carrier cooling reverses the initial exciton transition red-shift and induces transmission near the band edge due to state filling and stimulated emission. Finally, 1–100 ps signals are dominated by reverse state filling due to non-geminate recombination. These results demonstrate that both inter-band and exciton absorptions are essential for unraveling photo-induced dynamics in these materials, and that insights obtained from many-body theoretical analysis of dynamic screening are essential for correctly assigning the recorded spectral evolution.

Introduction

Organic lead halide perovskite (OLHP) semiconductors (SCs) are a promising family of photovoltaic materials.[1–5] Once deposited on inert porous solids, they present all of the essential functions required for producing a solar cell, and can be processed by solution phase chemistry at low cost. Those functions include strong absorption of visible to NIR light, efficient separation of the resulting excitons into free carriers, and spatial segregation of the holes and electrons. Remarkably, all of these functions which are commonly performed by several components are provided here by a single material. This unique combination of properties has allowed perovskite based solar cells to reach a power conversion efficiency (PCE) of up to 20% making them strong contenders for construction of next generation affordable photovoltaic devices.

The OLHPs are described as hybrid materials that combine both organic and inorganic molecular characteristics. The inorganic part of the perovskite structure contains sheets of corner-sharing metal halide octahedra, in which a divalent metal cation allows the balancing of charge. This framework bound by strong bonds of combined covalent and ionic characters is suggested to be responsible for the high carrier mobilities reported in the literature, and is connected with the large measured charge carrier diffusion lengths.[6–9] On the other hand, the organic part composed of single or double layers of organic cations (*e.g.* methyl-ammonium) enables the simplicity of deposition and low temperature processing. Another interesting feature of organo-metal perovskites is the ability to tune their optical band gap (BG) by altering the halides in the perovskite structure. For example, Noh *et al.* chemically exchanged iodide to bromide at differing mole fractions (*e.g.* $CH_3NH_3PbI_xBr_{3-x}$, where $0 \leq x \leq 3$) and observed substantial modifications in the optical properties of the material.[10] Mosconi *et al.* have performed theoretical modeling to explore the influences of halide exchange on the electronic properties of the lead based perovskites. Their periodic DFT calculated band structures are in accordance with the experimental trend of optical band gaps in these perovskite structures.[11] The tuning effect of the halide is assigned to the significant contribution of the halide p orbitals to the valence band while the conduction band is essentially metal ion based.[12] As Br (4p) is lower in energy than iodine 5p, the absorption onset in $CH_3NH_3PbI_xBr_{3-x}$ shifts to higher energies as x is decreased.[13]

The mechanisms which underlie OLHP's remarkable combination of photo-physical traits have been investigated

Institute of Chemistry, The Hebrew University, Jerusalem 91904, Israel. E-mail: sandy@mail.huji.ac.il

† Electronic supplementary information (ESI) available. See DOI: 10.1039/c5ta09643j

using ultrafast spectroscopy.[8,14–22] Pump-probe spectroscopy in the ps to nsec range was performed to test whether the diffusion lengths observed reflect transport by excitons, free carriers, or a combination of both. The results show that free carrier motions dominate high mobilities in this material, and that balanced contributions are made to charge transport by both conduction and valence bands. Due to this high mobility, non-geminate recombination of carriers competes effectively with other recombination processes even at relatively low carrier densities.

At even earlier times, pump-probe spectroscopy can reveal the crucial stages of exciton dissociation, and hot carrier relaxation, which set the stage for the subsequent transport. Beginning in the 1980s hot carrier relaxation in bulk SCs has been studied by femtosecond laser pump-probe methods.[23–26] The picture which has emerged from this effort is complex and includes numerous and sometimes opposing effects on the optical energy gap, transition strengths, and broadening of inter-band and exciton transitions. Photo-induced mobile carriers screen the Coulomb interactions between valence electrons and the lattice cores. This screening affects the absorption of the sample first by causing shrinkage of the gap between the valence and conduction bands which is coined BG renormalization. It reduces the Rydberg energy of Wannier excitons lying below the Band Edge (BE), and strongly damps the dipole strength of transitions to these bound states. The free carrier screening also reduces Coulomb enhancement of inter-band transitions, to a degree which is greatest at the BE, and which tapers off gradually as the probe frequency increases.[27,28] Finally, the highly polarizable excess charges tend to enhance dephasing rates of optical coherences leading to line broadening in sharp optical features such as the excitonic resonances.[29] All of the above strongly affect the intense and narrow transitions to exciton states, leading to pronounced TA features surrounding the BE even when pumping high above this level.[30] Finally, the photo-excited carriers affect absorption of the sample by virtue of their blocking states which were before free to contribute to inter-band absorption *i.e.* by state filling. This blocking effect will follow the process of relaxation of the hot carriers but is most apparent upon thermalization to the BG due to DOS considerations.

Sub-picosecond pump-probe data in OLHP samples following the above bandgap excitation revealed a number of distinct dynamic spectral features.[17,19,22] The most prominent is the rapid appearance of an intense Photo-Induced Bleach (PIB) centered at the optical band-edge which grows and broadens with increasing pump fluence. Another is the presence of a short lived Photo-Induced Absorption (PIA) band just below the optical BE which decays within a picosecond or so. The third is a broad and shallow PIA well above the band gap which grows in intensity and shifts to higher probe wavelengths over tens of picoseconds.

Interpretation of these features however varies broadly between the different reports. The below BG PIA was assigned by some to bi-exciton interactions, with its sub-ps disappearance attributed to dissociation of the nascent excitons.[14,22] This interpretation has been strengthened by direct ultrafast conduction measurements which suggest that photoexcitation at the BE leads to appearance of free carriers in ~2 ps.[15,31] Yet others have assigned the BE PIA to shifts in the absorption band to Wannier exciton states due to free hot carriers, with its disappearance accordingly due to cooling to the band edge.[19]

As for the BE PIB, it has been mainly assigned to state filling, with nearly no reference to screening effects on Sommerfeld enhancement of inter-band and exciton transitions. In particular the one study which explicitly considered many-body effects on the pump-probe data reports a gradual buildup of this BE bleach when it is excited above the BG, allegedly proving that this feature can be attributed to gradual state filling of the critical point by cooling of the initially hot free carriers.[19] In summary, despite the reasonable similarity of observations, drastically different dynamic scenarios are suggested to explain them.

Here we present an ultrafast TA study of hot exciton relaxation in organic–inorganic lead bromide and iodide perovskites at room temperature. In view of studies demonstrating similarities in the electronic structure and photophysics of both materials,[32] the tri-bromide is studied along with the photovoltaically relevant triiodide due to its mid-visible BG and excitonic structure which are convenient for full resolution of dynamic spectral changes surrounding the BE. Ultrafast pump-probe experiments were conducted on both materials prepared as thin films grown on flat glass substrates, allowing TA to concentrate on carrier dynamics without the added complications related to charge injection at the solid–solid interface. The results show that the above BG excitation of very low carrier densities leads to partial bleaching and spectral red shifting of the sharp Wannier exciton transition. At wavelengths significantly above the BE a concomitant weak and broad induced absorption also appears within ~130 fs. As demonstrated with global kinetic analysis, within a few hundred fs a rapid blue shifting of the same exciton transition takes place reflecting free carrier cooling. As the pump fluence is increased, a broadening of the exciton absorption as well as additional bleaching near the BE due to state filling becomes more and more prominent.

Analysis of the data demonstrates the need for including the effect of the excited free carriers on Coulomb enhancement of both inter-band and excitonic transitions, as well as the buildup of optical gain below the band edge upon exciton cooling. Finally, after the first ps or two, the effects of carrier recombination on the transient absorption are observed, to a degree which increases rapidly with the carrier density. We suggest that these screening effects along with state filling are sufficient to explain all of the above observations, and intra-band transitions are not obviously called for.

Methods

$MAPbI_3$ and $MAPbBr_3$ ($MA = CH_3NH_3$) samples were prepared upon a glass substrate by performing a two-step deposition. In the first step, 1 M solution of PbI_2 or $PbBr_2$ in dimethylformamide (DMF) was deposited upon the glass through spin coating, followed by annealing the samples for 30 minutes at 90 degree celsius. Then the PbI_2 and $PbBr_2$ samples were immersed in MAI or MABr solution in isopropanol (10.0 mg ml^{-1} for MAI and

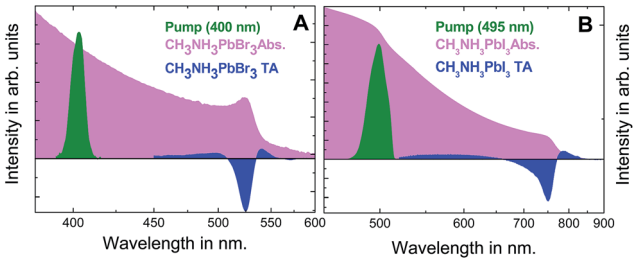

Fig. 1 Spectroscopic details of the experiments, including steady state absorption spectra of both samples, along with the pump pulses used to excite them, and TA spectra obtained at a pump-probe delay of 250 fs.

7.04 mg ml^{-1} for MABr), respectively, followed by annealing the samples for 30 minutes at 90 °C. The MAI and MABr were synthesized as detailed elsewhere.[33] SEM images of the samples along with their absorption and PL spectra are included in the ESI† online.

All pump probe experiments were carried out on a home built multi-pass amplified Ti:sapphire system generating 30 fs 790 nm pulses. 400 nm pump pulses were obtained by SHG in 100 μm of BBO. 500 nm pump pulses were obtained by mixing of the signal and fundamental in a TOPAS parametric amplifier (Light Conversion Ltd.). Probe pulses extending from 450 to 850 nm were generated by focusing ~1 μJ of the fundamental (790 nm) in 2.5 mm of sapphire. This was separated into probe and reference beams. The latter was collimated and refocused into the perovskite samples using only reflective optics. Both probe and reference beams were detected using a UV/Vis double diode array spectrograph. Sample absorption overlaid with 250 fs TA curves is presented with the laser intensity spectra of MABr and MAI samples in Fig. 1 panels A and B respectively. For additional experimental details see ref. 34.

Results

Fig. 2 and 3 present time corrected pump-probe data for excitation of tri-iodide and tri-bromide samples at 400 and 500 nm, respectively, and at three pump fluences differing by more than a factor of 20. Left panels describe the spectral increase over the initial 100–200 fs, while the right panels report later changes up to 100 ps. Data presented to the left pertains partly to pump-probe temporal overlap, and as addressed below, could thus include nonlinear coupling effects.

In both compounds a series of common trends are observed in line with previous studies of $MAPbI_3$ ultrafast photophysics. Despite the large excess photon energies (0.8 and 0.6 eV for the iodide and bromide, respectively) an immediate red shifting and partial bleaching of the band edge exciton transition are observed. A sub-picosecond stage of blue shifting of this feature follows which is blended with the buildup of stimulated emission below the BG. This spectral shifting is almost twice as fast in the tri-bromide, which also exhibits a much shallower net emission after it is over. Finally an increase in pump fluence progressively broadens all spectral features with a particular

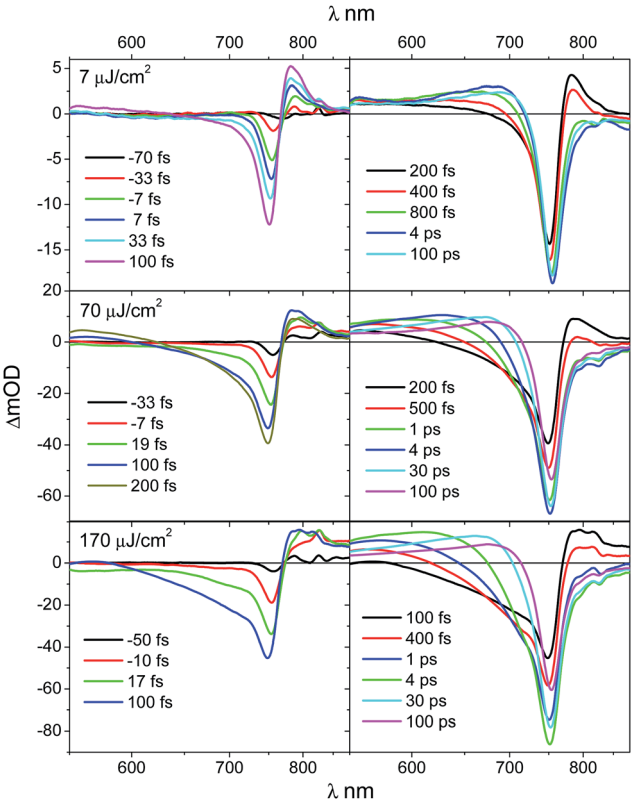

Fig. 2 Transient absorption spectra of $MAPbI_3$ films on optical glass after photoexcitation with 500 nm femtosecond pulses at 3 different fluences. See text for details.

effect on those related to the exciton transition including its initial bleaching, spectral red shifting, and a subsequent reverse shift to the blue. Increased pump intensity also leads to a saturation of the exciton band bleaching and to an extension of the prompt PIB which tails higher in the inter-band absorption range. Both these contributions to excess transmission are observable at all the tested pump fluences in the iodide, and remain distinct in the transient spectra throughout the 0.3–1 ps range. This distinctness will play a significant part in our interpretation of these results. Following these changes a much slower narrow and ultimate amplitude reduction in the prominent band edge bleach is observed for all but the lowest excitation intensities, and more so as the intensity is increased. This phase is faster when the pump intensity is higher, and matches earlier assignments to non-geminate carrier recombination. We stress that although more than half of the eV of excess energy is departed on tri-iodide samples, this energy falls below the second BE observed near 470 nm in the iodide.

Two measures are extracted from the data to aid in assigning these changes. Finite difference spectra and band integrals covering the probed spectral range were calculated.[35] The former is defined as: $\Delta\Delta\mathrm{OD}(\lambda,t,\Delta t)\equiv\Delta\mathrm{OD}\left(\lambda,t+\frac{\Delta t}{2}\right)-\Delta\mathrm{OD}\left(\lambda,t-\frac{\Delta t}{2}\right)$ which resolves spectral changes taking place over limited intervals of time, allowing isolated viewing of particular processes which are separable either due to their consecutive

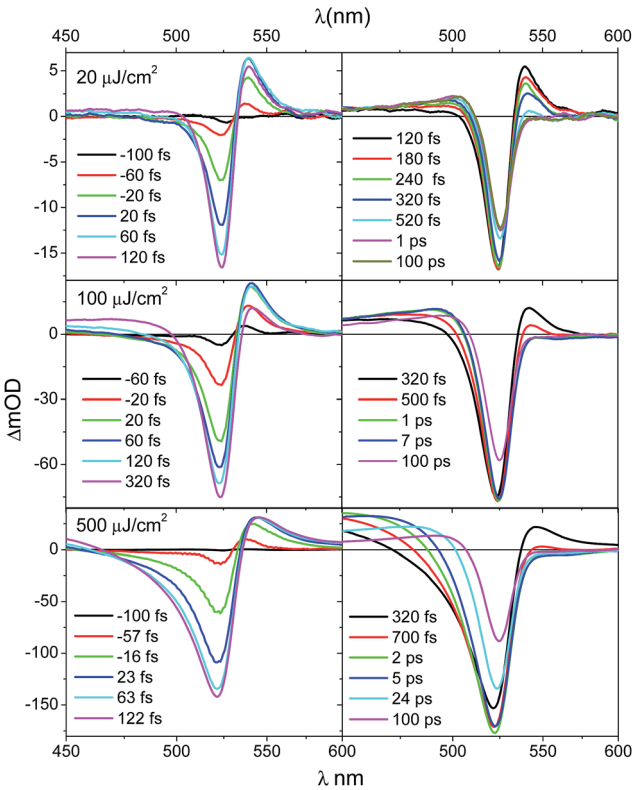

Fig. 3 Transient absorption spectra of $MAPbBr_3$ films on optical glass after photoexcitation with 400 nm femtosecond pulses at 3 different fluences.

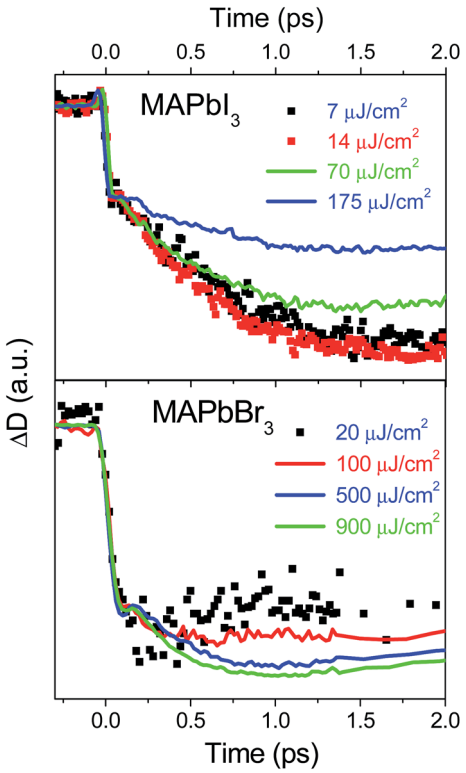

Fig. 4 Difference in the dipole strength over the whole measured spectrum calculated from data presented in Fig. 2 and 3.

nature, or by virtue of very different associated rates. The resulting finite difference spectra are presented in Fig. 5. The band integrals: $\Delta D \equiv \int \frac{\Delta OD}{\nu} d\nu$ in contrast cover changes in dipole strength of all transitions within the spectral range covered by the probe, allowing the separation of population variations from spectral shifts which redistribute but do not change the total dipole strength.[19,35]

The band integrals related to the data in Fig. 2 and 3 are presented in Fig. 4, revealing that in both materials, and at all investigated pump intensities, the initial response of the system is an ultrafast reduction in dipole strength across the probing range which is limited by the instrument response function. Also, in thin films of both materials this is nearly always followed by an additional fall in dipole strength over longer delays which roughly coincides with the band edge blue shifting described above. In both samples and at all pump intensities, the amplitude of the sharp drop in dipole strength is a significant fraction of the maximal reduction. It is however a much larger fraction in bromide, where the negative band integral increases by no more than 20% utmost, and at the lowest fluence it actually decays over the first ~1.5 ps. One question arising from this result is with regard to the mechanism of this initial bleaching which increases instantaneously, much faster than the expected relaxation time of hot carriers to the BE.

Turning to finite difference spectra in Fig. 5, spectral evolution of $MAPbBr_3$ at the lowest pump intensity is misleadingly simple. It can be modeled adequately as a machine limited partial bleach and red-shift of a sharp peak at the BG, followed by its exponential shift to the blue on a timescale of ~250 fs. Only magnification of the ΔOD scale reveals that excitation also leads to a shallow absorption extending to higher photon frequencies, and an equally shallow excess bleach just below the BE is leftover after the rapid shifting. Comparison of this panel with the associated band integral in Fig. 4 indicates that the delayed spectral evolution over the first picosecond or two consists mainly of spectral shifts with minimal changes in the total dipole strength. As the pump fluence is increased the BE bleach broadens asymmetrically to the blue, and the subsequent shifting feature exhibits massive broadening. Its zero crossing evolves to the red with time, and gives way continuously to a localized erasure of the initial bleach which continues far beyond the initial spectral shifting. A comparison with the tri-iodide shows a qualitative similarity in trends. Two main differences are that the range of asymmetric broadening of BE induced transmission is more extensive in the iodide, making it appear distinct from the contribution from the narrow exciton transition. The other is that the rapid blue-shift is markedly slower in $MAPbI_3$. To demonstrate this, global kinetic fitting was conducted on the lowest intensity experiments in both samples, assuming a single step kinetic scheme with finite temporal resolution and a Gaussian instrument response. The results presented in Fig. S1 of the ESI† supports the characterization of spectral shifting in $MAPbI_3$ and $MAPbBr_3$ on timescales of ~0.5 and ~0.25 ps, respectively.

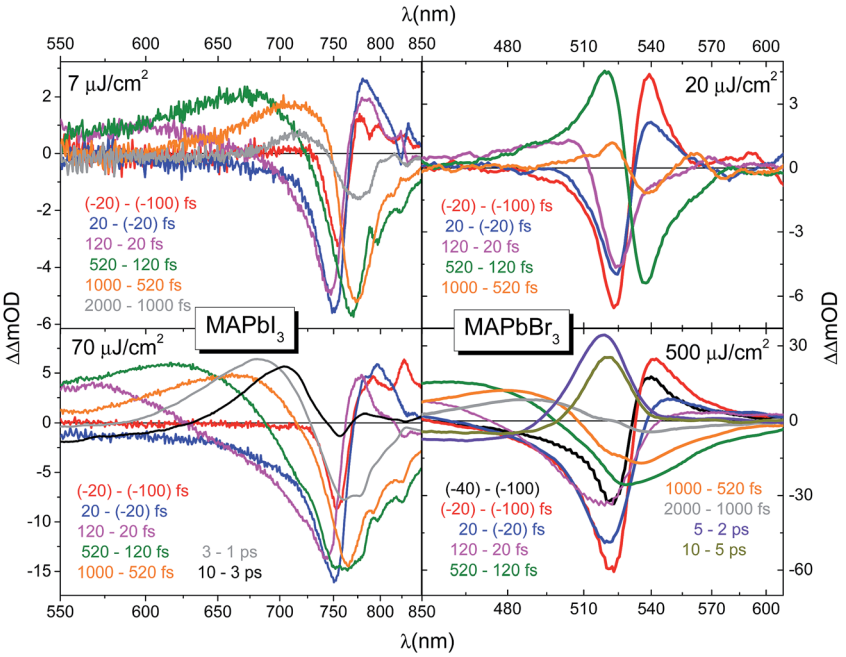

Fig. 5 Finite difference spectra calculated from the data represented in Fig. 2 and 3. Upper and lower panels present low and high fluence experiments, respectively. The left two panels present tri-iodide results, with the left showing spectra calculated for the tri-bromide.

Discussion

Previous studies have highlighted the roles of band filling and spectral shifting of excitonic bands in the ultrafast spectroscopy of OLHPs. However, the extreme promptness of pump induced BE bleaching poses a challenge to this view. With the current setup all stages of hot carrier relaxation following photo-absorption should be resolvable. We start assigning these spectral variations by first examining their sum total. After photo-generated carriers have relaxed and accumulated at the BE, three longer lived spectral features endure, an asymmetric BE bleach arising steeply on the red side and tailing to the blue, a gradual and smooth transition from this bleach to a shallow absorption further to the blue, and a shallow band of enhanced transmission below the BE.

The latter is most likely the signature of stimulated emission, in accordance with the known fluorescence spectrum of the perovskite films (see ESI† for emission curves from the samples studied).[20] Assignment of the former two bands is less straightforward. The intense BE bleach must reflect some band filling after carrier cooling. It could also result in part from reduced Coulomb enhancement of excitons as well as inter-band transitions near the BG. The broad absorption which develops to the blue of the BE bleach most likely reflects BG renormalization due to dynamic screening by the photo-generated carriers. A reduction of the BG will red-shift the inter-band and exciton transitions. As linear absorption increases monotonically above the BG, renormalization would result in a broad increase in extinction, with induced absorptions just below the BE. The latter is not observed in the data at long delays. We note that the broad absorption in the visible range has been assigned to intra-band transitions by Trinh *et al.* The intensity (intra-band transitions are formally forbidden), frequency and increased kinetics of this feature all argue against it. In particular, the kinetic correlation suggested in ref. 19 is not exhibited by our data.

As the pump intensity and carrier density grow, defining when thermalization is complete and delineating it from recombination become more difficult. Most published studies suggest that carrier cooling rates depend primarily on pump photon energy. However, Chen *et al.* present TA data in mixed halide perovskite films after high intensity photo-excitation well above the BE.[22] Their results show concomitant narrowing and deepening of the BE bleach with nothing even resembling an isosbestic point. Accordingly they invoke prolonged carrier thermalization which overlaps and mixes with fast carrier recombination at these densities. In our data this trend is absent as demonstrated in Fig. 2, 3, and S2† which present post-cooling TA data. Panel (a) shows how after the initial cooling the process of carrier recombination not only affects the depth of bleach but significantly narrows this feature, and its zero crossing wavelength, in accordance with the Moss–Burstein analysis presented by Kamat and co-workers.[17] Panels (b) and (c) present TA curves in iodide and bromide films, respectively, for different pump fluences and different probe delays such that the depth of BE bleach has reached the same amplitude. Clearly at this stage of spectral evolution the spectrum's shape and amplitude are perfectly correlated, indicating no memory of the initial excess pump energy, with the sole factor determining TA spectra being the remaining carrier density.

Dynamics which lead up to this ultimate difference spectrum include two distinct steps. The first is the apparently

instantaneous difference spectrum induced by the pump. The second, taking place over the first picosecond or so of delay is associated in our interpretation with hot carrier cooling. In particular the appearance of this phase of relaxation even after the above BE excitation which falls below the higher BE matches this assignment. At the lowest pump intensities, the spectral signatures throughout these early stages appear to stem exclusively from transitions to exciton states. Consisting of spectral shifting and bleaching, the near perfect odd and even parity of these contributions about the unperturbed BE, respectively (see Fig. 3), indicates that their source is a line spectrum and not a band edge – whose spectrum roughly resembles a step function.

Interestingly, the bandwidth of the sharp bleach which dominates difference spectra at low fluence in both samples is $\sim$600 cm^{-1}, which is not limited by the spectrograph resolution. It is a measure of the exciton absorption width in the unexcited solid. The bleach component to the immediate difference spectrum can be assigned to a screening induced fall in Coulomb enhancement of the exciton transition dipole,[27] as well as broadening of the exciton absorption band due to enhanced dipole dephasing. The initial red-shift shows that once excited, residual absorption to the sharp exciton peak shifts to lower energies. We note in passing that this red-shift appears only when the photon energy is in considerable excess of the optical BG. For this reason its assignment must be to the interaction of the exciton state with free carriers and not correlated pairs as previously suggested.

Why the first response of the exciton transition to hot carriers is a red-shift must depend on the balance between BG renormalization, and screening induced shrinking of the Rydberg constant. However, for this interpretation to hold, and given the amplitude of the spectral shift observed, the binding energy of the Wannier excitons must be at the tens of meV level. Reviewing the literature, estimates for this energy vary over two orders of magnitude from $\sim$80 to $\sim$2 meV,[9,16,32,36–39] and are predicted to depend critically on sample temperature. In light of our above interpretations, the correct value is in between these limits. In particular, the suggestion that the binding energy is only 1–2 meV, *i.e.* only KT/10@300 K would suggest dephasing times on the femtosecond timescale, producing much heavier broadening of the exciton transition.

As pump intensity is increased, the prompt bleaching signal at the BE saturates and extends to the blue. The saturation of the sharp exciton bleach probably reflects a strong dependence of the transition dipole on screening. We reiterate that pumping is far above the BG, requiring significant loss of excess energy from carriers in the conduction as well as valence bands before the BE states are blocked. Accordingly extension of the bleach to the blue may result from screening induced reduction of Coulomb enhancements to inter-band transitions, predicted to effect transitions up to $\sim 20XE_B$ above the BE, where E_B is the binding energy of the exciton.[28] Using this measure an estimated E_B for both materials would be in the range of 20–30 meV. This estimate is based on many-body theoretical analysis of femtosecond pump-probe experiments on various bulk SC materials, which indicates their generic applicability to the case at hand. It is also encouraging that a similar E_B of the iodide was recently obtained by fitting the steady state absorption spectrum at various temperatures with the Elliot theory.[40] The appearance of this broadening only at high pump intensities would indicate that the inter-band transition dipole depends more weakly on screening than the exciton transition.

An alternative explanation of the prompt broadening of the BE bleach to the blue at high fluence is that at least part of the state filling is taking place much faster than expected. Experiments reported here were conducted with relatively fine temporal resolution, and for band filling to seem instantaneous in our data would indicate carrier occupation of BG states within no more than $\sim$20 fs. In addition, a significant sub-ps phase of spectral evolution which has been assigned in earlier studies to hot carrier cooling is observed on a much longer timescale. We note that the signature of state filling is usually influenced by relaxations in both valence and conduction bands. Only experiments with even higher temporal resolution can decide if indeed at least one of these manifolds is conducive of such rapid thermalization.[41]

The duration of sub-ps blue shifting of the BE bleach is nearly unaffected by changes in pump fluence. In contrast, the spectral signature is very sensitive to carrier density, reflecting a rapid broadening of the exciton transition with the introduction of free carriers to the lattice. Broadening of transitions to exciton states due to carrier induced dephasing is a well-known consequence of photoexcitation in bulk SCs.[25–30] Increased pump intensity also leads to deviation from a simple "two state" spectral shift scenario to continuous spectral evolution, as demonstrated by the continuous variation of zero crossing in the finite difference spectra in Fig. 4. Aside from the added effects of non-geminate recombination, this probably includes the buildup of stimulated emission. The assignment of the latter is based on a comparison of the first few ps of spectral change in the iodide and bromide samples. Stimulated emission is far more prominent in TA spectra of the former, and so is the deviation from a simple spectral shift signature. How to factor in stimulated emission features will require further study of these samples. It is important to point out that absorption bleaching plays a much more predictable and prominent role than stimulated emission in TA from "hot" bulk SC samples. The latter requires a *k*-space correlation of the unbound and independently thermalizing holes and electrons. Accordingly emission from hot carriers in bulk SCs is weak and spectrally diffuse.[23] The former requires no such correlation, *i.e.* state filling in either conduction or valence bands can block transitions and induce bleaching signals. Emission thus contributes significantly only after overall cooling and even then to a lesser extent.

Conclusions

Ultrafast exciton dynamics in $CH_3NH_3PbI_3$ and $CH_3NH_3PbBr_3$ films is followed by tunable pump – hyperspectral probe spectroscopy. Significant excess energy was deposited in the perovskite films by pumping high in the inter-band continuum. As seen in other bulk semiconducting materials, analysis of the data reveals that in both samples photoexcitation leads to

prompt bleaching near the absorption edge. Visualizing these trends was facilitated by extracting finite difference spectra and band integrals. At low pump fluence the prompt spectral response comprises partial bleaching and red shifting of transitions to exciton states, subsequent blue shifting of which dominates sub-picosecond hot carrier thermalization. All of these spectral changes are dominated by the band edge exciton transitions demonstrating their hypersensitivity to the presence of photo-generated excess free carriers. Increased pump intensity saturates the exciton bleach and increasingly induces broad and asymmetric reduction in inter-band absorption. Like the exciton transition bleach, this is attributed to reduced Coulomb enhancement due to hot carrier screening. These assignments demonstrate that both inter-band and exciton absorptions are essential for unraveling photo-induced dynamics in these materials. They suggest significant binding energies of several tens of meV for excitons in both materials. Following cooling, 1–100 ps signals are dominated by non-geminate recombination, and in the case of the iodide, by the buildup of stimulated emission. In particular our results do not support earlier suggestions that at high exciton densities carrier thermalization can extend to tens of ps, and our reading of the data is that thermalization times are primarily dictated by the pump photon's excess energy above the optical band gap.

Acknowledgements

S. R., the Lester Aronberg Chair in applied chemistry, acknowledges support from the Israel Science Foundation, and the Binational Science Foundation. L. E. acknowledges financial support from the Israel Alternative Energy Foundation (I-SAEF). V. S. thanks the Lady Davis foundation for a post-doctoral fellowship.

References

1 M. Grätzel, *Nat. Mater.*, 2014, **13**, 838–842.
2 M. A. Green, A. Ho-Baillie and H. J. Snaith, *Nat. Photonics*, 2014, **8**, 506–514.
3 M. M. Lee, J. Teuscher, T. Miyasaka, T. N. Murakami and H. J. Snaith, *Science*, 2012, **338**, 643–647.
4 A. Kojima, K. Teshima, Y. Shirai and T. Miyasaka, *J. Am. Chem. Soc.*, 2009, **131**, 6050–6051.
5 J. Gong, S. B. Darling and F. You, *Energy Environ. Sci.*, 2015, **8**, 1953–1968.
6 S. D. Stranks, G. E. Eperon, G. Grancini, C. Menelaou, M. J. P. Alcocer, T. Leijtens, L. M. Herz, A. Petrozza and H. J. Snaith, *Science*, 2013, **342**, 341–344.
7 C. Wehrenfennig, G. E. Eperon, M. B. Johnston, H. J. Snaith and L. M. Herz, *Adv. Mater.*, 2014, **26**, 1584–1589.
8 G. Xing, N. Mathews, S. Sun, S. S. Lim, Y. M. Lam, M. Grätzel, S. Mhaisalkar and T. C. Sum, *Science*, 2013, **342**, 344–347.
9 A. Marchioro, J. Teuscher, D. Friedrich, M. Kunst, R. van de Krol, T. Moehl, M. Grätzel and J.-E. Moser, *Nat. Photonics*, 2014, **8**, 250–255.
10 J. H. Noh, S. H. Im, J. H. Heo, T. N. Mandal and S. I. Seok, *Nano Lett.*, 2013, **13**, 1764–1769.
11 E. Mosconi, A. Amat, M. K. Nazeeruddin, M. Grätzel and F. de Angelis, *J. Phys. Chem. C*, 2013, **117**, 13902–13913.
12 N. Kitazawa, *Mater. Sci. Eng., B*, 1997, **49**, 233–238.
13 T. Ishihara, *J. Lumin.*, 1994, **60–61**, 269–274.
14 F. Deschler, M. Price, S. Pathak, L. E. Klintberg, D.-D. Jarausch, R. Higler, S. Hüttner, T. Leijtens, S. D. Stranks, H. J. Snaith, M. Atatüre, R. T. Phillips and R. H. Friend, *J. Phys. Chem. Lett.*, 2014, **5**, 1421–1426.
15 C. S. Ponseca, T. J. Savenije, M. Abdellah, K. Zheng, A. Yartsev, T. Pascher, T. Harlang, P. Chabera, T. Pullerits, A. Stepanov, J.-P. Wolf and V. Sundström, *J. Am. Chem. Soc.*, 2014, **136**, 5189–5192.
16 T. J. Savenije, C. S. Ponseca, L. Kunneman, M. Abdellah, K. Zheng, Y. Tian, Q. Zhu, S. E. Canton, I. G. Scheblykin, T. Pullerits, A. Yartsev and V. Sundström, *J. Phys. Chem. Lett.*, 2014, **5**, 2189–2194.
17 J. S. Manser and P. V. Kamat, *Nat. Photonics*, 2014, **8**, 737–743.
18 J. A. Christians, J. S. Manser and P. V. Kamat, *J. Phys. Chem. Lett.*, 2015, **6**, 2086–2095.
19 M. T. Trinh, X. Wu, D. Niesner and X.-Y. Zhu, *J. Mater. Chem. A*, 2015, **3**, 9285–9290.
20 X. Wu, M. T. Trinh, D. Niesner, H. Zhu, Z. Norman, J. S. Owen, O. Yaffe, B. J. Kudisch and X.-Y. Zhu, *J. Am. Chem. Soc.*, 2015, **137**, 2089–2096.
21 L. Wang, C. McCleese, A. Kovalsky, Y. Zhao and C. Burda, *J. Am. Chem. Soc.*, 2014, **136**, 12205–12208.
22 K. Chen, A. J. Barker, F. L. C. Morgan, J. E. Halpert and J. M. Hodgkiss, *J. Phys. Chem. Lett.*, 2015, **6**, 153–158.
23 J. Shah, *Ultrafast spectroscopy of semiconductors and semiconductor nanostructures*, Springer Science & Business Media, 1999, vol. 115.
24 A. Othonos, *J. Appl. Phys.*, 1998, **83**, 1789–1830.
25 Y. H. Lee, A. Chavez-Pirson, S. W. Koch, H. M. Gibbs, S. H. Park, J. Morhange, A. Jeffery, N. Peyghambarian, L. Banyai, A. C. Gossard and W. Wiegmann, *Phys. Rev. Lett.*, 1986, **57**, 2446–2449.
26 J. Shah, R. F. Leheny and W. Wiegmann, *Phys. Rev. B: Solid State*, 1977, **16**, 1577.
27 R. J. Elliott, *Phys. Rev.*, 1957, **108**, 1384.
28 H. Haug and S. W. Koch, *Phys. Rev. A*, 1989, **39**, 1887–1898.
29 Y. Masumoto, B. Fluegel, K. Meissner, S. W. Koch, R. Binder, A. Paul and N. Peyghambarian, *J. Cryst. Growth*, 1992, **117**, 732–737.
30 J. Nunnenkamp, J. H. Collet, J. Klebniczki, J. Kuhl and K. Ploog, *Phys. Rev. B: Condens. Matter Mater. Phys.*, 1991, **43**, 14047.
31 D. A. Valverde-Chávez, C. S. Ponseca, C. C. Stoumpos, A. Yartsev, M. G. Kanatzidis, V. Sundström and D. G. Cooke, *Energy Environ. Sci.*, 2015, **8**, 3700–3707.
32 K. Tanaka, T. Takahashi, T. Ban, T. Kondo, K. Uchida and N. Miura, *Solid State Commun.*, 2003, **127**, 619–623.
33 S. Aharon, B. E. Cohen and L. Etgar, *J. Phys. Chem. C*, 2014, **118**, 17160–17165.
34 J. Zhu, I. Gdor, E. Smolensky, N. Friedman, M. Sheves and S. Ruhman, *J. Phys. Chem. B*, 2010, **114**, 3038–3045.
35 I. Gdor, A. Shapiro, C. Yang, D. Yanover, E. Lifshitz and S. Ruhman, *ACS Nano*, 2015, **9**, 2138–2147.

36 V. D'Innocenzo, G. Grancini, M. J. P. Alcocer, A. R. S. Kandada, S. D. Stranks, M. M. Lee, G. Lanzani, H. J. Snaith and A. Petrozza, *Nat. Commun.*, 2014, **5**, 3586.
37 A. Miyata, A. Mitioglu, P. Plochocka, O. Portugall, J. T.-W. Wang, S. D. Stranks, H. J. Snaith and R. J. Nicholas, *Nat. Phys.*, 2015, **11**, 582–587.
38 K. Zheng, Q. Zhu, M. Abdellah, M. E. Messing, W. Zhang, A. Generalov, Y. Niu, L. Ribaud, S. E. Canton and T. Pullerits, *J. Phys. Chem. Lett.*, 2015, **6**, 2969–2975.
39 Q. Lin, A. Armin, R. C. R. Nagiri, P. L. Burn and P. Meredith, *Nat. Photonics*, 2015, **9**, 106–112.
40 M. Saba, M. Cadelano, D. Marongiu, F. Chen, V. Sarritzu, N. Sestu, C. Figus, M. Aresti, R. Piras, A. G. Lehmann, C. Cannas, A. Musinu, F. Quochi, A. Mura and G. Bongiovanni, *Nat. Commun.*, 2014, **5**, 5049.
41 A. Kahan, O. Nahmias, N. Friedman, M. Sheves and S. Ruhman, *J. Am. Chem. Soc.*, 2007, **129**, 537–546.